

Product Datasheet

UFL1 Antibody NBP1-79039

Unit Size: 0.1 ml

Store at 4C. Do not freeze.

www.novusbio.com



technical@novusbio.com

Publications: 3

Protocols, Publications, Related Products, Reviews, Research Tools and Images at:
www.novusbio.com/NBP1-79039

Updated 9/9/2025 v.20.1

Earn rewards for product
reviews and publications.

Submit a publication at www.novusbio.com/publications

Submit a review at www.novusbio.com/reviews/destination/NBP1-79039



NBP1-79039

UFL1 Antibody

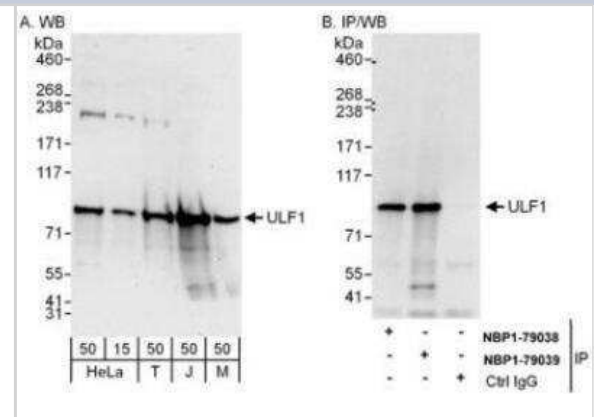
Product Information	
Unit Size	0.1 ml
Concentration	0.2 mg/ml
Storage	Store at 4C. Do not freeze.
Clonality	Polyclonal
Preservative	0.09% Sodium Azide
Isotype	IgG
Purity	Immunogen affinity purified
Buffer	TBS and 0.1% BSA

Product Description	
Description	Novus Biologicals Rabbit UFL1 Antibody (NBP1-79039) is a polyclonal antibody validated for use in WB and IP. Anti-UFL1 Antibody: Cited in 2 publications. All Novus Biologicals antibodies are covered by our 100% guarantee.
Host	Rabbit
Gene ID	23376
Gene Symbol	UFL1
Species	Human, Mouse
Immunogen	The immunogen recognized by this antibody maps to a region between residue 744 and 794 of human E3 UFM1-Protein Ligase 1 using the numbering given in entry NP_056138.1 (GeneID 23376).

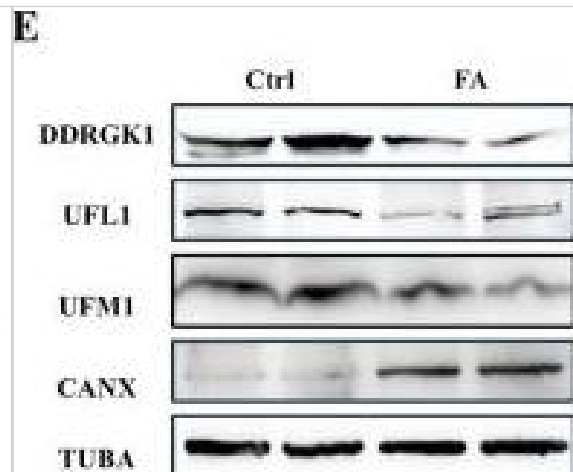
Product Application Details	
Applications	Western Blot, Immunoprecipitation
Recommended Dilutions	Western Blot 1:2000-1:10000, Immunoprecipitation 2-10 ug/mg
Application Notes	Western blot of lysates performed using standard western blot reagents and 4-8% SDS-PAGE.

Images

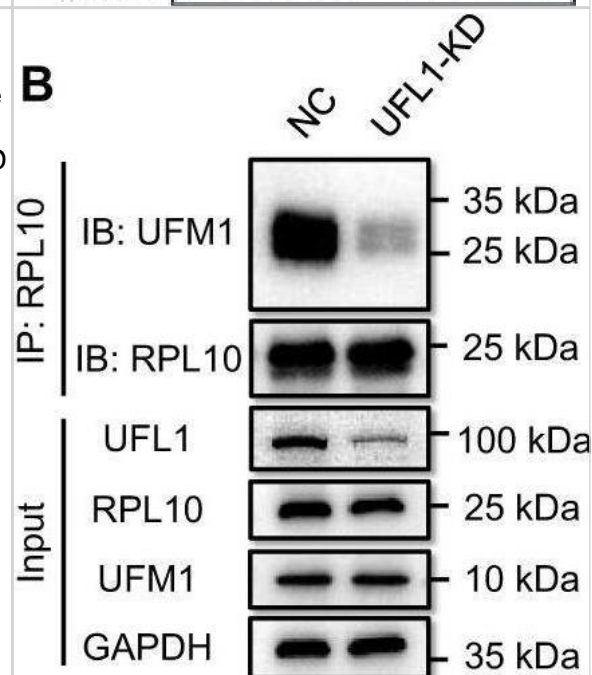
Western Blot: UFL1 Antibody [NBP1-79039] - Whole cell lysate from HeLa (15 and 50 mcg for WB; 1 mg for IP, 20% of IP loaded), 293T (T; 50 mcg), Jurkat (J; 50 mcg) and mouse NIH3T3 (M; 50 mcg) cells. Antibodies: Affinity purified rabbit anti-UFL1 antibody used for WB at 0.04 mcg/ml (A) and 0.4 mcg/ml (B) and used for IP at 6 mcg/mg lysate. UFL1 was also immunoprecipitated by rabbit anti-UFL1 antibody NBP1-79038 which recognizes an upstream epitope.



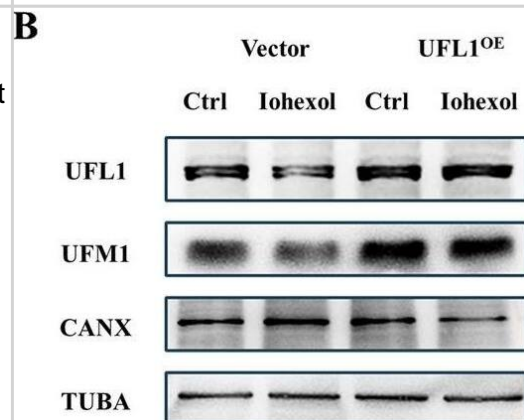
Folic acid suppresses ER-phagy, worsening ER stress, and apoptosis. A Diagrammatic representation of FA mice (250 mg/kg) and control mice. The renal function was evaluated by serum creatinine (B) and BUN (C). D Representative histology of HE and PAS staining in the renal cortex. Scale bar: 500 μ m and 50 μ m. E–I The immunoblot analysis and quantification of DDRGK1, UFL1, UFM1, and CANX in kidney lysates. J TEM images of ER in renal tubular epithelial cell. Red arrows: ER. K–M The immunoblot analysis and quantification of GRP78 and CHOP in kidney lysates. N, O The immunoblot analysis and quantification of BAX in kidney lysates. Data are presented as the mean \pm SEM (n = 5). **p < 0.01 and ***p < 0.001. Image collected and cropped by CiteAb from the following open publication (<https://pubmed.ncbi.nlm.nih.gov/38233375>), licensed under a CC-BY license. Not internally tested by Novus Biologicals.



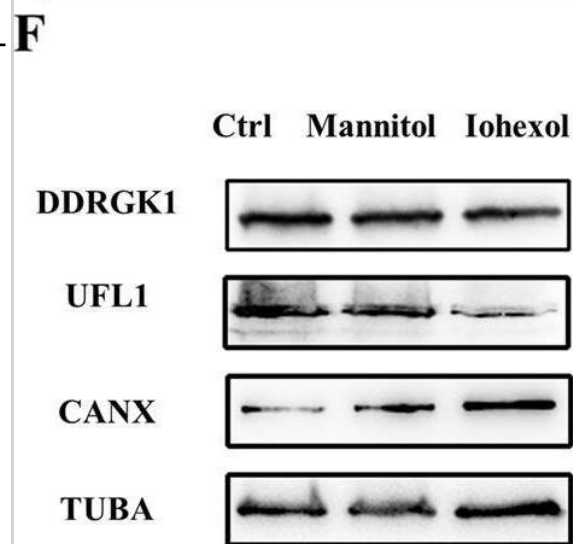
Confirmation of the involvement of UFL1 and UFSP2 in RPL10 ufmylation and the effect on pancreatic cancer cells. A Direct binding of RPL10 and UFL1 in PANC-1 cells was detected by Co-IP. B The change of RPL10 ufmylation was detected by after UFL1 silencing in PANC-1 cells. C Direct binding of UFSP2 and RPL10 in PANC-1 cells by Co-IP. D The change of RPL10 ufmylation after overexpressing UFSP2 in PANC-1 cells. E The proliferations of PANC-1 cells and Mia PaCa-2 cells after silencing UFL1. The proliferations were detected by CCK-8 method (n = 10). F The proliferations of PANC-1 and Mia PaCa-2 cells after overexpressing UFSP2. The proliferation rates were detected by CCK-8 method (n = 10). G The colony formation of PANC-1 and Mia PaCa-2 cells after silencing UFL1. The colonies were stained with crystal violet and analyzed (n = 3). H The colony formation of PANC-1 and Mia PaCa-2 cells after overexpressing UFSP2. The colonies were stained with crystal violet and analyzed (n = 3). All experiments were independently repeated for 3 times, and the data are expressed as mean \pm SD. *P < 0.05 indicates statistically significant versus negative control. **P < 0.01 indicates statistically very significant versus negative control. Image collected and cropped by CiteAb from the following open publication (<https://pubmed.ncbi.nlm.nih.gov/37280198>), licensed under a CC-BY license. Not internally tested by Novus Biologicals.



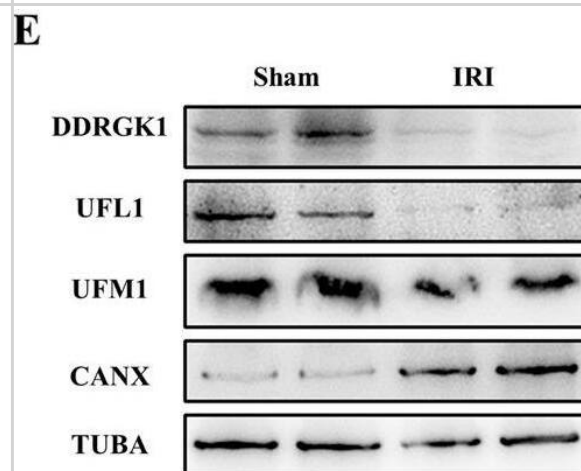
UFL1 overexpression rescues ER-phagy and mitigates ER stress and apoptosis. UFL1 plasmid was transfected to HK-2 cells to overexpress UFL1. A CCK-8 assay of UFL1 overexpression HK-2 cells with or without Iohexol. B–D The immunoblot analysis and quantification of UFL1, UFM1, and CANX in cell lysates. E–G The immunoblot analysis and quantification of GRP78 and CHOP in cell lysates. H, I The immunoblot analysis and quantification of BAX in cell lysates. Data are presented as the mean \pm SEM (n = 3). *p < 0.05, **p < 0.01 and ***p < 0.001. Image collected and cropped by CiteAb from the following open publication (<https://pubmed.ncbi.nlm.nih.gov/38233375>), licensed under a CC-BY license. Not internally tested by Novus Biologicals.



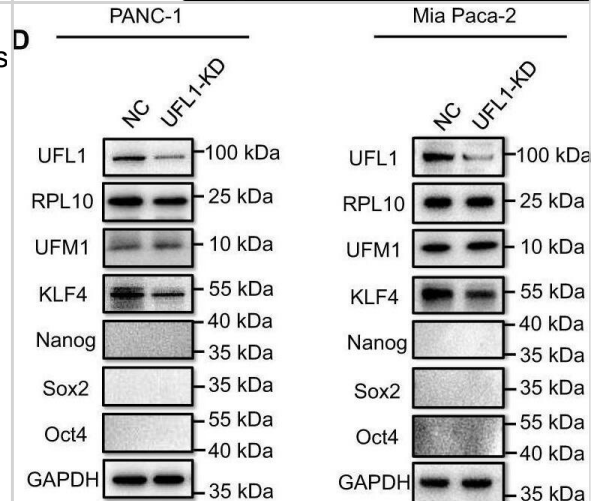
In vitro CI-AKI model shows reduced ER-phagy. HK-2 cells were incubated in DMEM/F12 containing Iohexol (150 mg l/ml) for 6 h. A CCK-8 assay of Iohexol-treated HK-2 cells, together with the isosmotic control group, mannitol-treated HK-2 cells. B, C Diagrammatic representation of the mCherry cleavage from ER assay. Briefly, degradation of ER resulted in the lysosomal cleavage of the mCherry tag from RAMP4, which caused a smaller, mCherry-only product to be resolved by immunoblot analysis. D Diagrammatic representation of ER-phagy tandem reporter assay. eGFP is quenched in lysosomal-induced low pH situations, causing GFP+/mCherry+ to GFP-/mCherry+ during ER-phagy. E The representative image of ER-phagy tandem reporter assay by confocal microscope. Scale bar: 5 μ m. White arrows: GFP-/mCherry+ puncta. F-I The immunoblot analysis and quantification of DDRGK1, UFL1, CANX in cell lysates. J-L The immunoblot analysis and quantification of GRP78 and CHOP in cell lysates. M, N The immunoblot analysis and quantification of BAX in cell lysates. Data are presented as the mean \pm SEM (n = 3). *p < 0.05, **p < 0.01 and ***p < 0.001. Image collected and cropped by CiteAb from the following open publication (<https://pubmed.ncbi.nlm.nih.gov/38233375>), licensed under a CC-BY license. Not internally tested by Novus Biologicals.



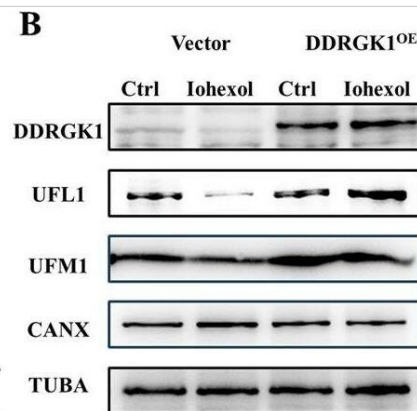
IRI inhibits ER-phagy, intensifying ER stress and apoptosis. A Diagrammatic representation of IRI mice (right nephrectomy and left kidney ischemia 30 min) and sham mice. The renal function was evaluated by serum creatinine (B) and BUN (C). D Representative histology of HE and PAS staining in the renal cortex. Scale bar: 500 μ m and 50 μ m. E-I The immunoblot analysis and quantification of DDRGK1, UFL1, UFM1, CANX in kidney lysates. J TEM images of ER in renal tubular epithelial cell. Red arrows: ER. K-M The immunoblot analysis and quantification of GRP78 and CHOP in kidney lysates. N, O The immunoblot analysis and quantification of BAX in kidney lysates. Data are presented as the mean \pm SEM (n = 5). ***p < 0.001. Image collected and cropped by CiteAb from the following open publication (<https://pubmed.ncbi.nlm.nih.gov/38233375>), licensed under a CC-BY license. Not internally tested by Novus Biologicals.



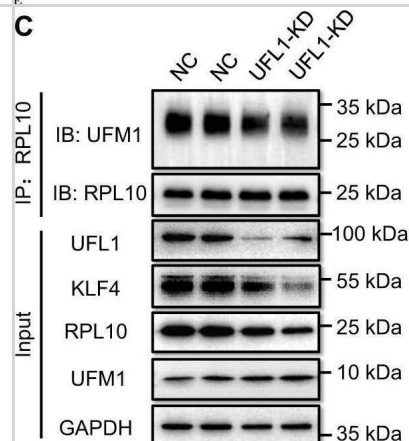
Identification of transcription factor KLF4 in PRL10 ufmylation related stemness of pancreatic cancer cells. A The correlation between stemness related transcription factors and UFM1 in tissues of PAAD patients (<http://gepia2.cancer-pku.cn/#correlation>). B The correlation between stemness related transcription factors and RPL10 in tissues of PAAD patients (<http://gepia2.cancer-pku.cn/#correlation>). C The relationship between the development of PAAD and gene transcripts of transcription factors (<http://gepia2.cancer-pku.cn/#analysis>). TPM is the abbreviation of transcripts per million of genes. D Protein expression of different transcription factors after the knockdown of UFL1 in PANC-1 and Mia PaCa-2 cells. E Protein expression of different transcription factors after the overexpression of UFSP2 in PANC-1 and Mia PaCa-2 cells. All experiments were independently repeated for 3 times. Image collected and cropped by CiteAb from the following open publication (<https://pubmed.ncbi.nlm.nih.gov/37280198>), licensed under a CC-BY license. Not internally tested by Novus Biologicals.



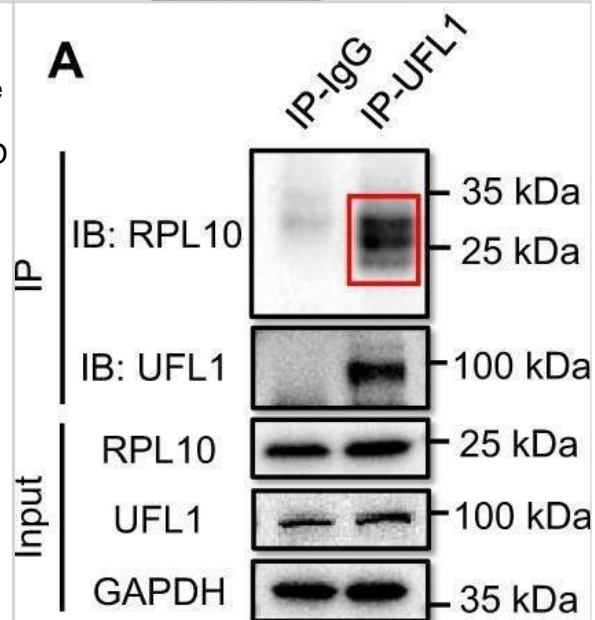
DDRGGK1 overexpression rescues ER-phagy and mitigates ER stress and apoptosis. DDRGGK1 plasmid was transfected to HK-2 cells to overexpress DDRGGK1. A CCK-8 assay of DDRGGK1 overexpression HK-2 cells with or without Iohexol. B–E The immunoblot analysis and quantification of DDRGGK1, UFL1, UFM1, CANX in cell lysates. F–H The immunoblot analysis and quantification of GRP78 and CHOP in cell lysates. I, J The immunoblot analysis and quantification of BAX in cell lysates. Data are presented as the mean \pm SEM (n = 3). *p < 0.05, **p < 0.01 and ***p < 0.001. Image collected and cropped by CiteAb from the following open publication (<https://pubmed.ncbi.nlm.nih.gov/38233375>), licensed under a CC-BY license. Not internally tested by Novus Biologicals.



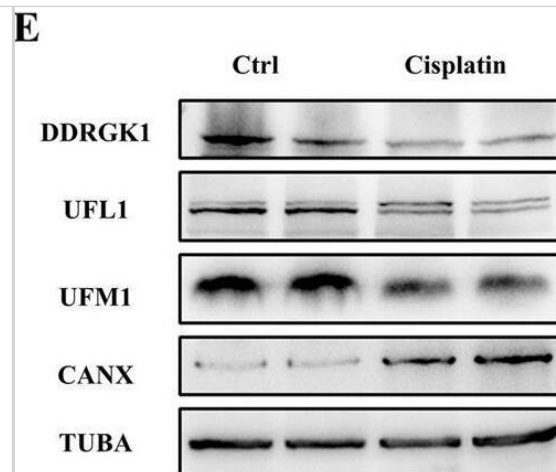
Confirmation of the involvement of UFL1 in tumorigenesis and cell stemness in vivo. A The effects of the knockdown of UFL1 on tumor growth. Each group contained 8 mice, and data are expressed as mean \pm SD. *P < 0.05 indicates statistically significant versus negative control. **P < 0.01 indicates statistically very significant versus negative control. B The effect of UFL1 knockdown on tumor growth by Ki67 staining. C Examination of RPL10 ufmylation and KLF4 expression in tumor tissues by Co-IP and WB. Tumor tissues were randomly chosen from each group. D The effects of the knockdown of UFL1 on cell stemness related markers by immunochemical staining. Image collected and cropped by CiteAb from the following open publication (<https://pubmed.ncbi.nlm.nih.gov/37280198>), licensed under a CC-BY license. Not internally tested by Novus Biologicals.



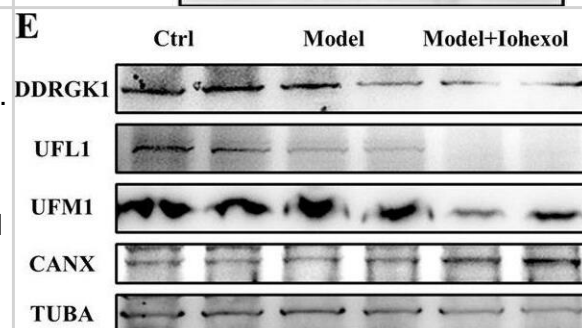
Confirmation of the involvement of UFL1 and UFSP2 in RPL10 ufmylation and the effect on pancreatic cancer cells. A Direct binding of RPL10 and UFL1 in PANC-1 cells was detected by Co-IP. B The change of RPL10 ufmylation was detected by after UFL1 silencing in PANC-1 cells. C Direct binding of UFSP2 and RPL10 in PANC-1 cells by Co-IP. D The change of RPL10 ufmylation after overexpressing UFSP2 in PANC-1 cells. E The proliferations of PANC-1 cells and Mia PaCa-2 cells after silencing UFL1. The proliferations were detected by CCK-8 method (n = 10). F The proliferations of PANC-1 and Mia PaCa-2 cells after overexpressing UFSP2. The proliferation rates were detected by CCK-8 method (n = 10). G The colony formation of PANC-1 and Mia PaCa-2 cells after silencing UFL1. The colonies were stained with crystal violet and analyzed (n = 3). H The colony formation of PANC-1 and Mia PaCa-2 cells after overexpressing UFSP2. The colonies were stained with crystal violet and analyzed (n = 3). All experiments were independently repeated for 3 times, and the data are expressed as mean \pm SD. *P < 0.05 indicates statistically significant versus negative control. **P < 0.01 indicates statistically very significant versus negative control. Image collected and cropped by CiteAb from the following open publication (<https://pubmed.ncbi.nlm.nih.gov/37280198>), licensed under a CC-BY license. Not internally tested by Novus Biologicals.



Cisplatin negatively regulates ER-phagy, heightening ER stress and apoptosis. A Diagrammatic representation of Cisplatin mice (20 mg/kg) and control mice. The renal function was evaluated by serum creatinine (B) and BUN (C). D Representative histology of HE and PAS staining in the renal cortex. Scale bar: 500 μ m and 50 μ m. E–I The immunoblot analysis and quantification of DDRGK1, UFL1, UFM1, and CANX in kidney lysates. J TEM images of ER in renal tubular epithelial cell. Red arrows: ER. K–M The immunoblot analysis and quantification of GRP78 and CHOP in kidney lysates. N, O The immunoblot analysis and quantification of BAX in kidney lysates. Data are presented as the mean \pm SEM (n = 5). **p < 0.01 and ***p < 0.001. Image collected and cropped by CiteAb from the following open publication (<https://pubmed.ncbi.nlm.nih.gov/38233375>), licensed under a CC-BY license. Not internally tested by Novus Biologicals.



Contrast media suppresses ER-phagy, exacerbating ER stress and apoptosis. A Diagrammatic representation of CI-AKI mice (Model + Iohexol, 10 ml/kg), negative control mice (Model + NS), and control mice. The renal function was evaluated by serum creatinine (B) and BUN (C). D Representative histology of HE and PAS staining in the renal cortex. Scale bar: 500 μ m and 50 μ m. E–I The immunoblot analysis and quantification of DDRGK1, UFL1, UFM1, CANX in kidney lysates. J TEM images of ER in renal tubular epithelial cell. Red arrows: ER. K–M The immunoblot analysis and quantification of GRP78 and CHOP in kidney lysates. N, O The immunoblot analysis and quantification of BAX in kidney lysates. Data are presented as the mean \pm SEM (n = 5). **p < 0.01 and ***p < 0.001. Image collected and cropped by CiteAb from the following open publication (<https://pubmed.ncbi.nlm.nih.gov/38233375>), licensed under a CC-BY license. Not internally tested by Novus Biologicals.



Publications

Schmidt H, Sorensen G, Lanahan M et al. UFMylation promotes orthoflavivirus infectious particle production Journal of Virology 2025-07-01 [PMID: 40459261]

Haijiao Jin, Yuanting Yang, Xuying Zhu, Yin Zhou, Yao Xu, Jialin Li, Chaojun Qi, Xinghua Shao, Jingkui Wu, Shan Wu, Hong Cai, Leyi Gu, Shan Mou, Zhaohui Ni, Shu Li, Qisheng Lin DDRGK1-mediated ER-phagy attenuates acute kidney injury through ER-stress and apoptosis Cell Death & Disease 2024-01-17 [PMID: 38233375]

Wang K, Chen S, Wu Y et al. The ufmylation modification of ribosomal protein L10 in the development of pancreatic adenocarcinoma Cell death & disease 2023-06-07 [PMID: 37280198] (WB, Mouse)



Novus Biologicals USA

10730 E. Briarwood Avenue
Centennial, CO 80112
USA
Phone: 303.730.1950
Toll Free: 1.888.506.6887
Fax: 303.730.1966
nb-customerservice@bio-techne.com

Bio-Techne Canada

21 Canmotor Ave
Toronto, ON M8Z 4E6
Canada
Phone: 905.827.6400
Toll Free: 855.668.8722
Fax: 905.827.6402
canada.inquires@bio-techne.com

Bio-Techne Ltd

19 Barton Lane
Abingdon Science Park
Abingdon, OX14 3NB, United Kingdom
Phone: (44) (0) 1235 529449
Free Phone: 0800 37 34 15
Fax: (44) (0) 1235 533420
info.EMEA@bio-techne.com

General Contact Information

www.novusbio.com
Technical Support: nb-technical@bio-techne.com
Orders: nb-customerservice@bio-techne.com
General: novus@novusbio.com

Products Related to NBP1-79039

NBP2-33376H	Blue Marker Antibody (6F4-F6) [HRP]
HAF008	Goat anti-Rabbit IgG Secondary Antibody [HRP]
NB7160	Goat anti-Rabbit IgG (H+L) Secondary Antibody [HRP]
NBP2-24891	Rabbit IgG Isotype Control

Limitations

This product is for research use only and is not approved for use in humans or in clinical diagnosis. Primary Antibodies are guaranteed for 1 year from date of receipt.

For more information on our 100% guarantee, please visit www.novusbio.com/guarantee

Earn gift cards/discounts by submitting a review: www.novusbio.com/reviews/submit/NBP1-79039

Earn gift cards/discounts by submitting a publication using this product:
www.novusbio.com/publications

